

Xianyong Cao | Ulrike Herzschuh | Jian Ni | Yan Zhao
Thomas Böhmer

Spatial and temporal distributions of major tree taxa in eastern continental Asia during the last 22,000 years

Suggested citation referring to the original publication:

The Holocene 25(1) (2015)

DOI <https://doi.org/10.1177/0959683614556385>

ISSN (print) 0959-6836

ISSN (online) 1477-0911

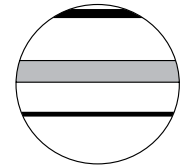
Postprint archived at the Institutional Repository of the Potsdam University in:

Postprints der Universität Potsdam


Mathematisch-Naturwissenschaftliche Reihe ; 417

ISSN 1866-8372

<http://nbn-resolving.de/urn:nbn:de:kobv:517-opus4-404174>



Spatial and temporal distributions of major tree taxa in eastern continental Asia during the last 22,000 years

The Holocene
2015, Vol. 25(1) 79–91
© The Author(s) 2015
Reprints and permissions:
sagepub.co.uk/journalsPermissions.nav
DOI: 10.1177/0959683614556385
hol.sagepub.com


Xianyong Cao,^{1,2} Ulrike Herzschuh,^{1,2} Jian Ni,^{1,2} Yan Zhao³
and Thomas Böhmer^{1,2}

Abstract

This study investigates the spatial and temporal distributions of 14 key arboreal taxa and their driving forces during the last 22,000 calendar years before AD 1950 (kyr BP) using a taxonomically harmonized and temporally standardized fossil pollen dataset with a 500-year resolution from the eastern part of continental Asia. Logistic regression was used to estimate pollen abundance thresholds for vegetation occurrence (presence or dominance), based on modern pollen data and present ranges of 14 taxa in China. Our investigation reveals marked changes in spatial and temporal distributions of the major arboreal taxa. The thermophilous (*Castanea*, *Castanopsis*, *Cyclobalanopsis*, *Fagus*, *Pterocarya*) and eurythermal (*Juglans*, *Quercus*, *Tilia*, *Ulmus*) broadleaved tree taxa were restricted to the current tropical or subtropical areas of China during the Last Glacial Maximum (LGM) and spread northward since c. 14.5 kyr BP. *Betula* and conifer taxa (*Abies*, *Picea*, *Pinus*), in contrast, retained a wider distribution during the LGM and showed no distinct expansion direction during the Late Glacial. Since the late mid-Holocene, the abundance but not the spatial extent of most trees decreased. The changes in spatial and temporal distributions for the 14 taxa are a reflection of climate changes, in particular monsoonal moisture, and, in the late Holocene, human impact. The post-LGM expansion patterns in eastern continental China seem to be different from those reported for Europe and North America, for example, the westward spread for eurythermal broadleaved taxa.

Keywords

China, Holocene, Last Glacial Maximum, pollen mapping, vegetation expansion

Received 20 April 2014; revised manuscript accepted 22 August 2014

Introduction

Determining the spatial distribution and temporal abundance changes of arboreal taxa during the late Quaternary is important for understanding present-day distributions of tree populations, and for interpreting the driving forces. Accordingly, it has been a focus of vegetation scientists for several decades. Vegetation change based on pollen-data mapping at a continental/sub-continental scale was first investigated for north-eastern North America (Bernabo and Webb, 1977) and Europe (Huntley and Birks, 1983). More recently, the European Pollen Database was used to locate potential glacial refugia for various trees and to reconstruct the subsequent migrational pathways to their current distributions (Brewer et al., 2002; Giesecke and Bennett, 2004; Van der Knaap et al., 2005). Works of comparable spatial extent and temporal and taxonomic resolution are currently lacking for the Asian continent.

The eastern part of continental Asia, the focus region of this study, encompasses various biomes reflecting large climate gradients. It has a long history of human civilization with potentially marked effects on vegetation distribution and taxa abundance (Gong et al., 2003; Li et al., 2009; Lu et al., 2009). The region is therefore a suitable area to study past natural and human-induced range and abundance changes for arboreal taxa.

Spatial distributions and temporal changes of key arboreal taxa from Asia have been investigated, for example, *Abies/Picea*,

Pinus, *Betula*, *Quercus* and *Ulmus* in China north of the Yangtze River (Ren and Beug, 2002; Ren and Zhang, 1998); *Picea* on the Loess Plateau (Zhou and Li, 2012); and *Alnus*, *Pinus* (Diploxy-lon) and *Quercus* on the southern Korean Peninsula (Yoon et al., 2011). Furthermore, Ren (2007) studied forest-cover changes in China north of the Yangtze River during the Holocene using a 40% threshold of arboreal pollen to map the forest-steppe boundary. However, the restricted spatial extent of the study areas means that these pioneering pollen-mapping studies are unable to provide a comprehensive picture of past vegetation changes beyond a regional scale.

In this paper, we estimate the pollen abundance thresholds of a taxon's presence/absence and dominance/presence by logistic

¹Alfred Wegener Institute Helmholtz Centre for Polar and Marine Research, Germany

²University of Potsdam, Germany

³Chinese Academy of Sciences, China

Corresponding author:

Xianyong Cao, Alfred Wegener Institute Helmholtz Centre for Polar and Marine Research, Research Unit Potsdam, Telegrafenberg A43, Potsdam 14473, Germany.
Email: Xianyong.Cao@awi.de; cxyhebtu@sohu.com

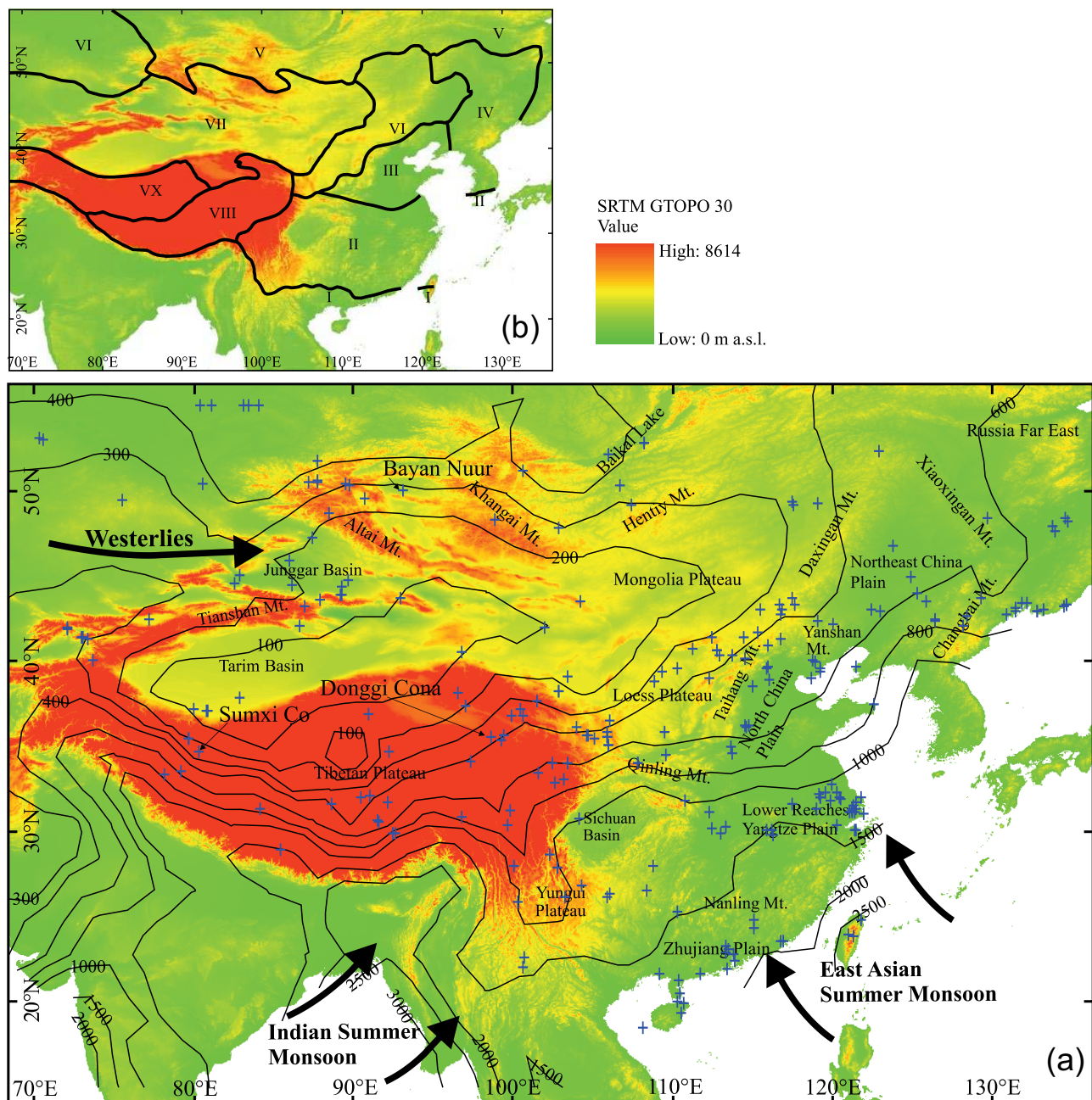


Figure 1. (a) Total annual precipitation (mm), climatic systems and main topographical units of the study area. (b) Modern vegetation zones. Vegetation zone map (modified from Hou (2001) and Olson et al. (2001)): I – tropical rainforest and seasonal rainforest; II – subtropical evergreen broadleaved forest; III – warm-temperate deciduous forest; IV – temperate mixed conifer–deciduous broadleaved forest; V – boreal conifer forest; VI – temperate steppe; VII – temperate desert; VIII – high-cold meadow and steppe; IX – high-cold semi-desert and desert. The contours of total annual precipitation have been interpolated by kriging in ArcMap 10, based on 2592 precipitation observations. Blue crosses indicate locations of available pollen records in the fossil pollen dataset (Cao et al., 2013) and the three new added records.

regression modelling based on the relationship between modern pollen abundances and corresponding plant distributions for 14 key arboreal pollen taxa (*Abies*, *Betula*, *Castanea*, *Castanopsis*, *Cyclobalanopsis*, *Fagus*, *Juglans*, *Larix*, *Picea*, *Pinus*, *Pterocarya*, *Quercus*, *Tilia*, *Ulmus*). We then apply these pollen abundance thresholds to fossil pollen records derived from a taxonomically harmonized and temporally standardized fossil pollen dataset from eastern continental Asia (Cao et al., 2013) and map the spatial distribution changes of the key arboreal taxa since the Last Glacial Maximum (LGM). Finally, we compare the obtained pattern of taxa changes to those inferred for North America and Europe to highlight regional peculiarities and synthesize the relevant information so as to glean from past changes a better understanding of likely tree distribution changes within the frame of recent climate change.

Regional setting

The study area encompasses China, Mongolia, south-eastern Siberia (Russia), eastern Kazakhstan and eastern Kyrgyzstan, with a latitudinal range from 18°N to 55°N and a longitudinal range from 70°E to 135°E (Figure 1).

The study area can be divided into three major geographical units (Figure 1a): (1) the eastern plains and lowlands (mainly below 500 m.a.s.l.), which have long histories of agriculture dating back to about 10 cal. kyr BP (Gong et al., 2003, 2007; Li et al., 2009; Lu et al., 2009); (2) the low plateaux and basin areas lie mainly between 1000 and 2000 m.a.s.l.; although these areas have long histories of civilization too, the natural vegetation has been less modified than on the eastern plains (Fu, 2003; Li et al., 2009);

Table 1. The presence/absence and dominance/presence thresholds of the 14 key arboreal taxa revealed by logistic regression of modern pollen percentages versus occurrence in the vegetation inferred from vegetation maps (Hou, 2001; Fang et al., 2011).

Pollen taxa	Presence								As dominant/indicative species		
	Probability								β -value of Wald test	Probability	β -value of Wald test
	0.3	0.4	0.5	0.6	0.7	0.8	0.9	0.5			
<i>Abies</i>	1.2	1.7	2	2.7	3	4	5	<0.001	6	<0.001	
<i>Betula</i>	–	–	–	3	6	10	16	<0.001	25	<0.001	
<i>Castanea</i>	1	3	5	6	8	10	14	<0.001	–	–	
<i>Castanopsis</i>	3	5	7	9	10	13	16	<0.001	10	<0.001	
<i>Cyclobalanopsis</i>	1	2.5	4	5	7	9	12	<0.001	25	<0.001	
<i>Fagus</i>	1	1.3	1.6	1.9	2.2	2.6	3.2	<0.001	–	–	
<i>Juglans</i>	0.2	0.3	0.5	0.6	0.8	1	1.3	<0.001	–	–	
<i>Larix</i>	0.2	0.5	0.8	1.1	1.5	1.9	2.5	<0.001	2	<0.001	
<i>Picea</i>	–	–	1	2	4	6	9	<0.001	18	<0.001	
<i>Pinus</i>	–	–	–	5	13	23	37	<0.001	20	<0.001	
<i>Pterocarya</i>	1	2	3	4	5	6	8	<0.001	–	–	
<i>Quercus</i>	–	2	6	10	15	21	30	<0.001	17	<0.001	
<i>Tilia</i>	0.1	0.4	0.7	1	1.5	2	3	<0.001	6	<0.001	
<i>Ulmus</i>	–	–	–	–	0.5	1	2	<0.001	–	–	

Bold type indicates the selected pollen percentage thresholds for mapping. The dash means no >0 threshold available for presence probability or no available present range as dominant/indicative species.

(3) the Tibetan Plateau with a mean elevation of over 4000 m.a.s.l.; human impact is largely limited to grazing in restricted areas.

Most of the Chinese territories and the southern part of the Russian Far East belong to an area influenced by the Indian Summer Monsoon and the East Asian Summer Monsoon. The climate of Mongolia, western Inner Mongolia, the north-western Tibetan Plateau and areas to their west is dominated by westerly circulation (Tao and Chen, 1987; Wang et al., 2010). There is a marked precipitation gradient from south-east China to the desert areas of central Asia (Figure 1a).

The vegetation zones in the eastern part of the study area consist of tropical rainforest and seasonal rainforest (south of ~23°N), subtropical evergreen broadleaved forest (23°N–32°N), warm-temperate deciduous forest (32°N–40°N), temperate mixed conifer–deciduous broadleaved forest (40°N–50°N) and boreal conifer forest (north of ~50°N). The natural vegetation, following the south-east–north-west precipitation gradient, changes from a moist coastal forest zone, to steppe to desert, reflecting increasing continentality. In the north-western part of the study area, alpine conifer forests occur in mountainous areas, with forest-steppe in northern Kazakhstan because of the relatively wet climatic conditions. Alpine vegetation zones on the Tibetan Plateau follow a southeast to northwest precipitation gradient from mountainous forest to high-cold meadow, high-cold steppe, semi-desert and high-cold desert (Hilbig, 1995; Hou, 2001; Figure 1b).

Data and methods

Modern pollen percentages (2434 sites) and present geographical ranges for the 14 key arboreal taxa from China were used in logistic regression modelling to estimate the pollen abundance threshold for a taxon's occurrence (presence or dominance) in the vegetation. These threshold values reflect pollen–vegetation relationships reasonably (pollen distributions with more than 0.5 probability generally coincide with present geographical ranges for most taxa) and are mostly in accordance with threshold values from previous studies (although *Pinus* and *Pterocarya* might be respectively under- and over-estimated). More detail on processing is provided in Appendix 1 (available online).

The taxonomically harmonized and temporally standardized fossil pollen dataset (Cao et al., 2013) was employed to investigate the distribution changes of the 14 arboreal taxa since 22 kyr BP at

a 500-year resolution in eastern continental Asia. For the 271 pollen records included in the dataset, pollen percentage was standardized (on the basis of the total number of terrestrial pollen grains, including Cyperaceae), pollen taxonomy was harmonized, age–depth relationships were established for 260 sites using Bacon software (Blaauw and Christen, 2011) and linear interpolation was used for 11 sites. Pollen abundances for each 500-year time slice were interpolated using the linear integration function of Analy-Series 2.0.4.2 (Paillard et al., 1996). More detail on processing is provided in Cao et al. (2013). In this study, we added three new pollen records: Lake Donggi Cona (35.5°N, 98.5°E, 4090 m.a.s.l.; Wang et al., 2014) from the eastern part of the Tibetan Plateau, Lake Sumxi Co (34.6°N, 84.2°E, 5059 m.a.s.l.; Campo and Gasse, 1993) from the western margin of the Tibetan Plateau, and Lake Bayan Nuur (90.9°N, 48.8°E, 1576 m.a.s.l.; Krengel, 2000) from north-west Mongolia. For this study, we evaluated the reliability of each age–depth model for all pollen records, and excluded 31 pollen records because of their low average frequency of dates (more than every 5 kyr) from pollen mapping. The 243 available pollen records cover the major vegetation zones in the study area.

We selected pollen abundance thresholds at high probabilities (0.5, 0.7 and 0.9 for taxon presence; 0.5 for taxon dominance; Table 1) to represent plant presence and/or dominance, and used the program ArcMap 10.1 to generate past plant distribution maps at each 500-year interval for the 14 arboreal taxa.

Results

The distribution maps for each taxon showing their presence/absence and dominance thresholds with different probabilities for each 500-year interval (Appendix 2, available online) show the spatial and temporal distribution changes (significantly or insignificantly) in different time slices. The distribution maps of the 14 arboreal pollen taxa at six key time slices (Figure 2) further clearly reveal their strong spatial and temporal changes. All ages are in calibrated years BP.

Thermophilous broadleaved tree taxa

Castanea (Chestnut). The distribution centre of chestnut trees is located in the middle and lower reaches of the Yangtze River. Chestnut trees were limited to the estuaries of the Yangtze River

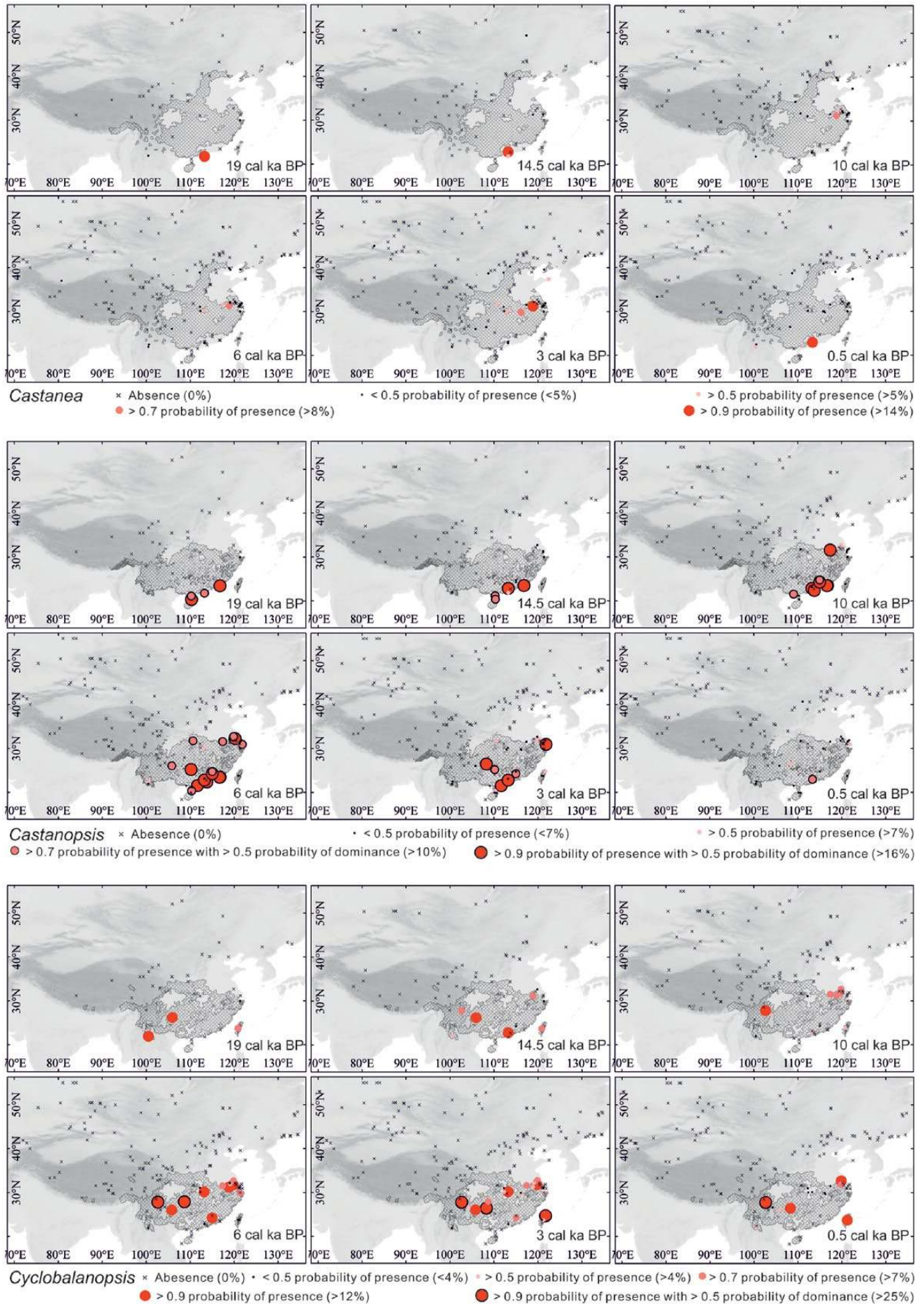
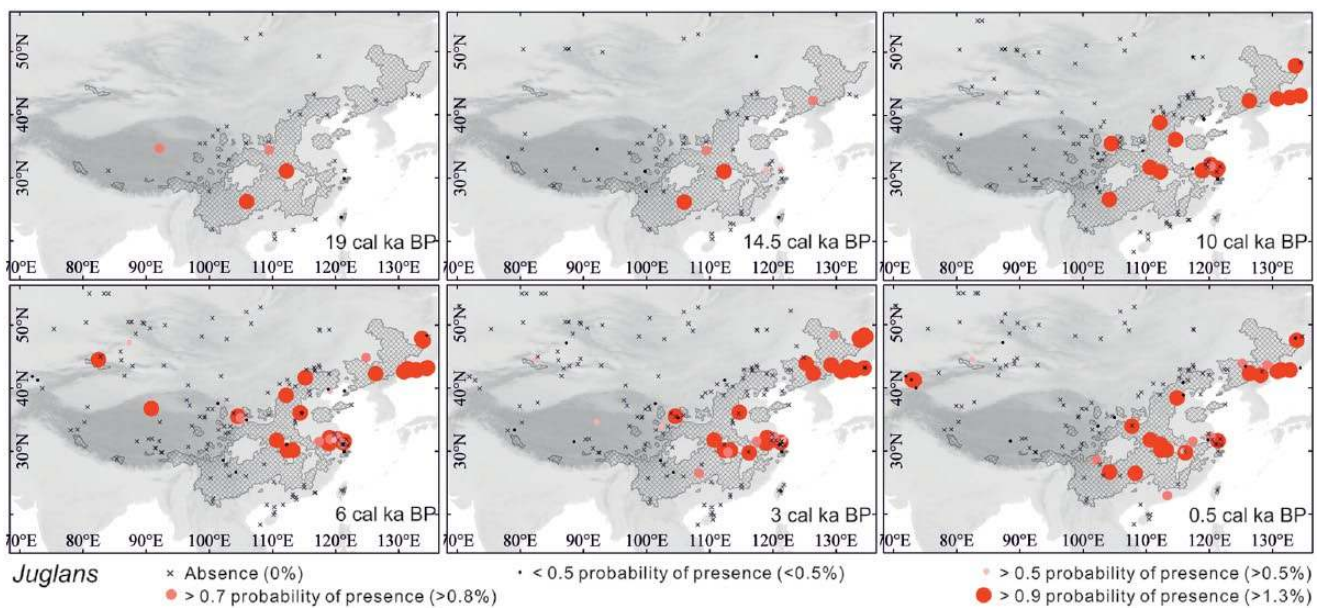
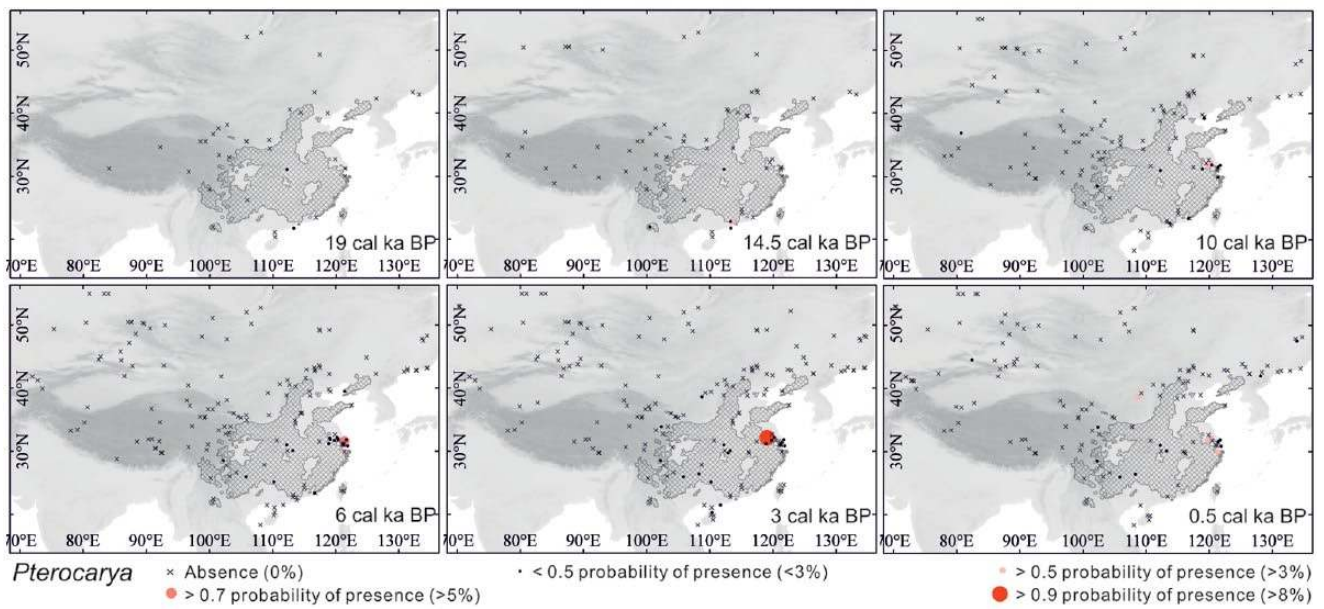
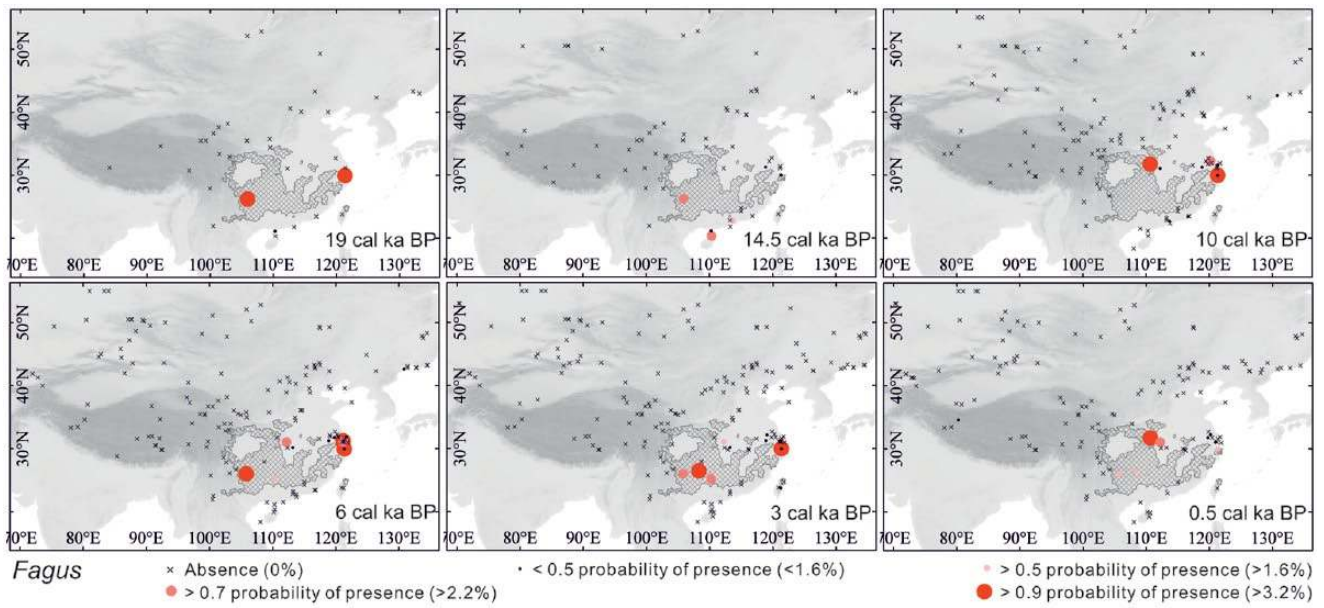
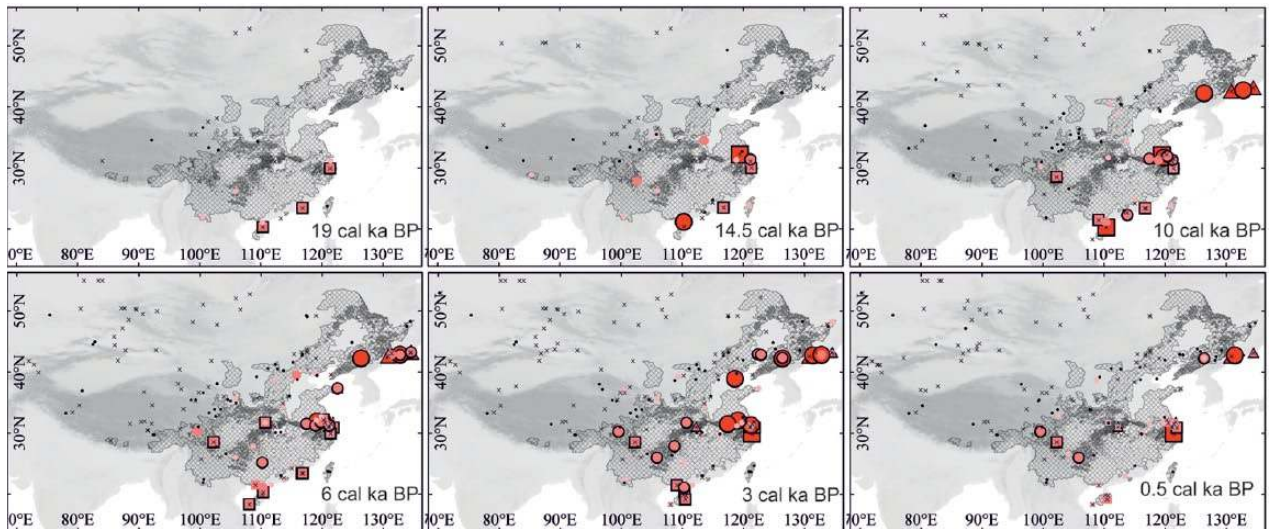


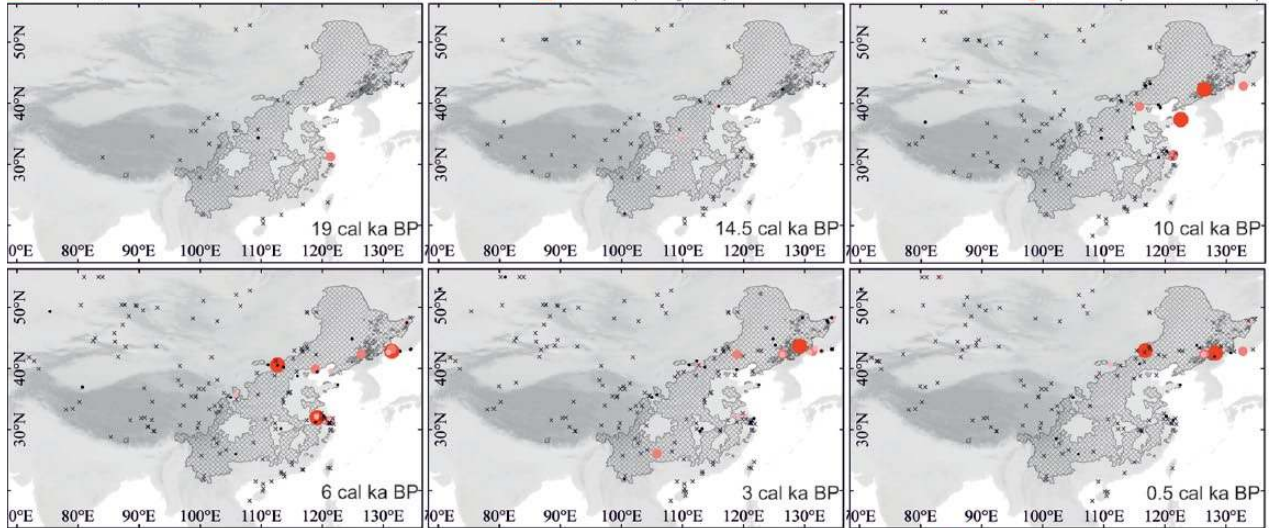
Figure 2. (Continued)



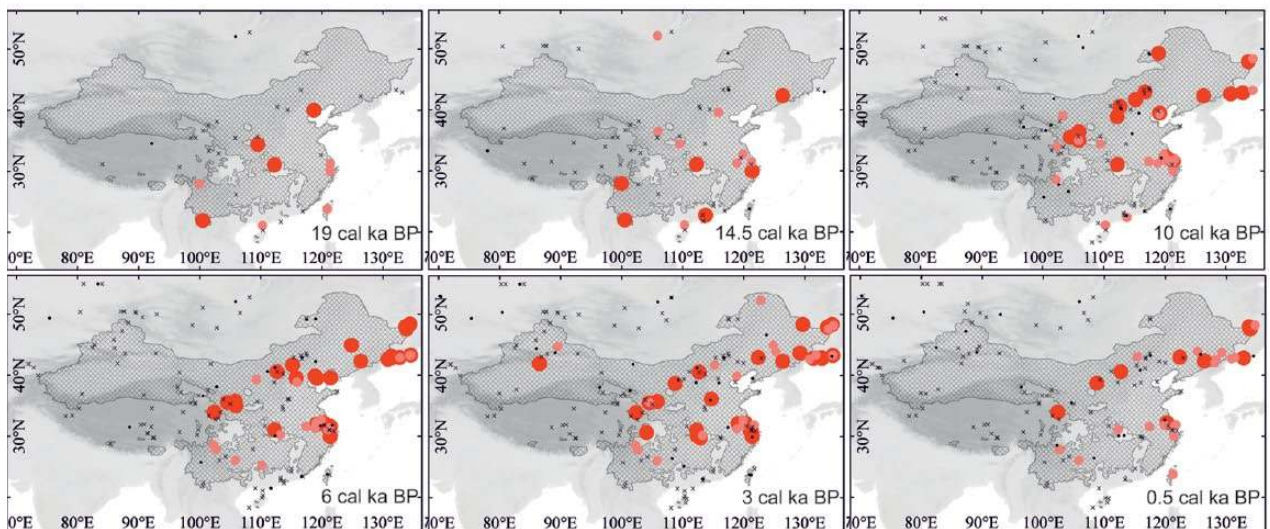
(Continued)



Quercus × Absence (0%) · < 0.5 probability of presence (<6%) ▲● > 0.5 probability of presence (>6%) ●● > 0.7 probability of presence (>15%)
 ▲●● > 0.7 probability of presence with > 0.5 probability of dominance (>17%) ▲●●● > 0.9 probability of presence with > 0.5 probability of dominance (>30%)
 ▲ *Quercus* (deciduous) ■ *Quercus* (evergreen) ● *Quercus* (undifferentiated)

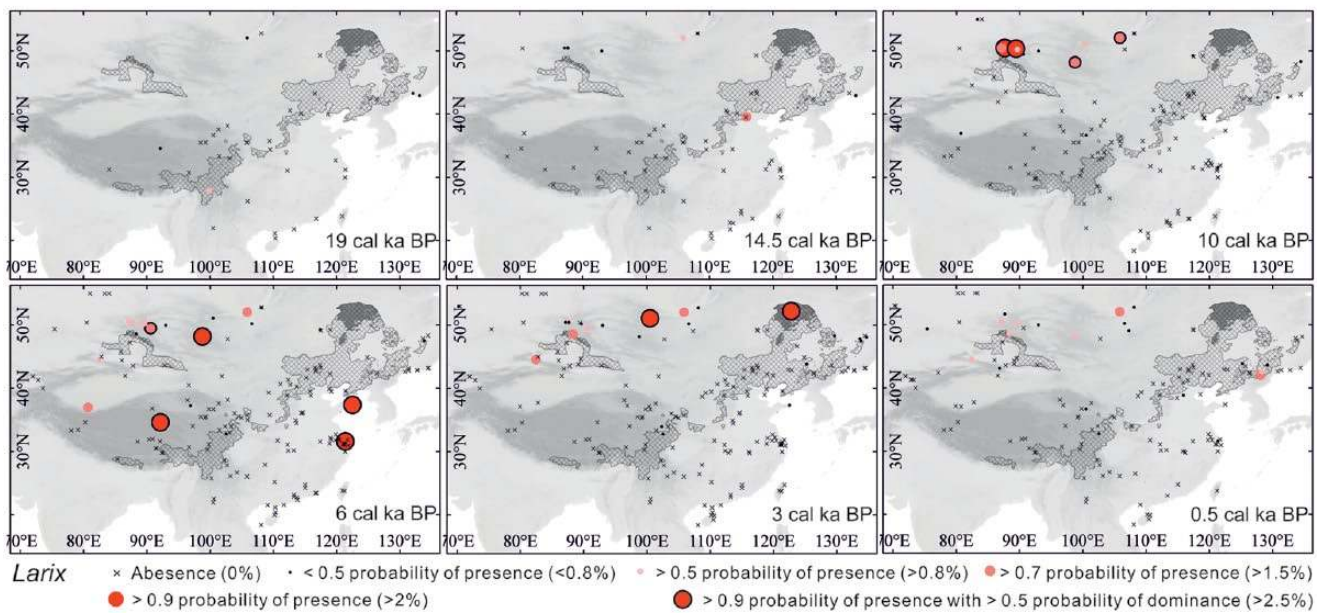
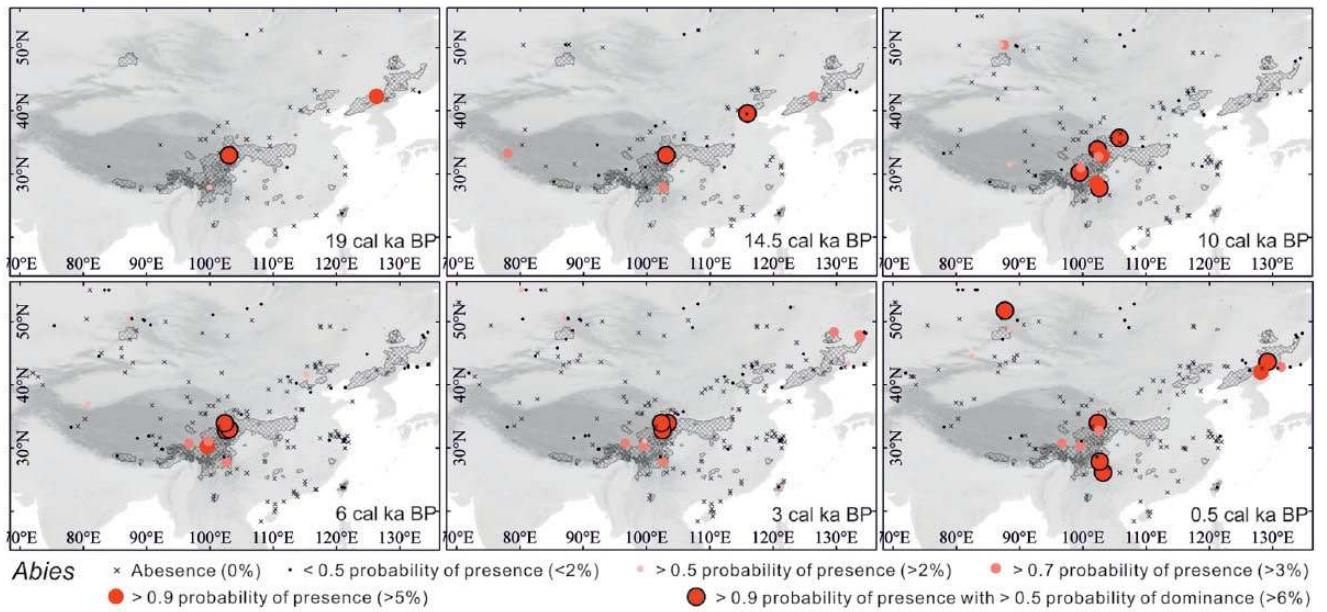
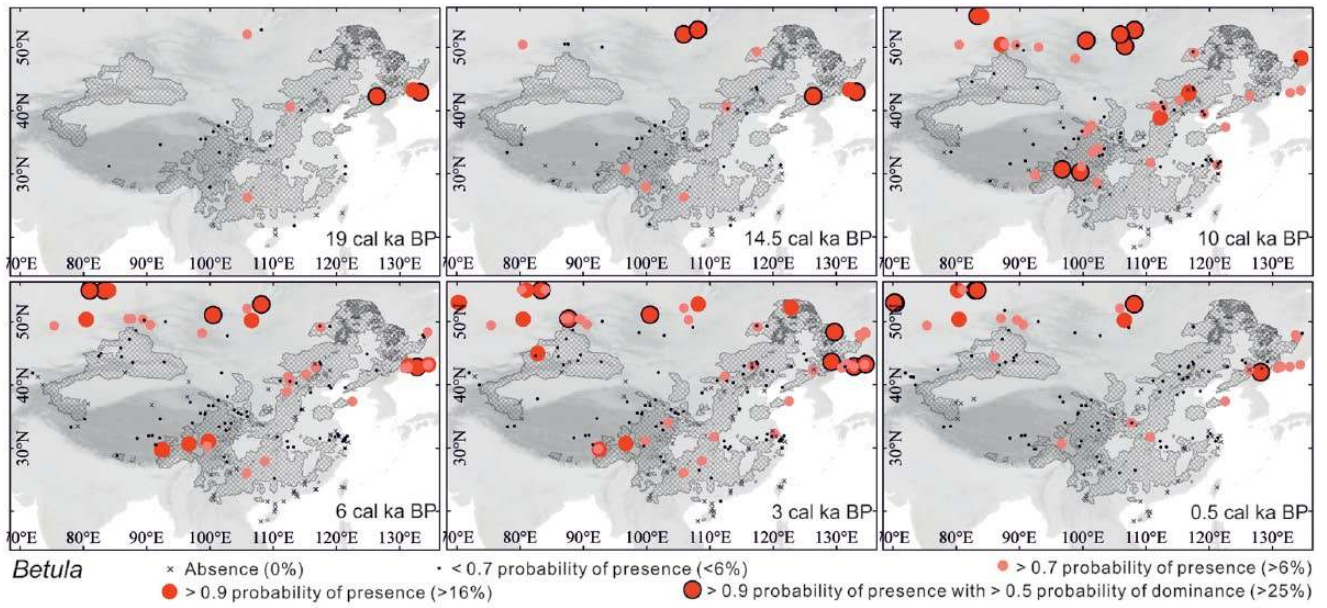


Tilia × Absence (0%) · < 0.5 probability of presence (<0.7%) ● > 0.5 probability of presence (>0.7%) ●● > 0.7 probability of presence (>1.5%)
 ●●● > 0.9 probability of presence (>3%) ●●●● > 0.9 probability of presence with > 0.5 probability of dominance (>6%)



Ulmus × Absence (0%) · < 0.7 probability of presence (<0.5%) ● > 0.7 probability of presence (>0.5%) ●●● > 0.9 probability of presence (>2%)

(Continued)



(Continued)

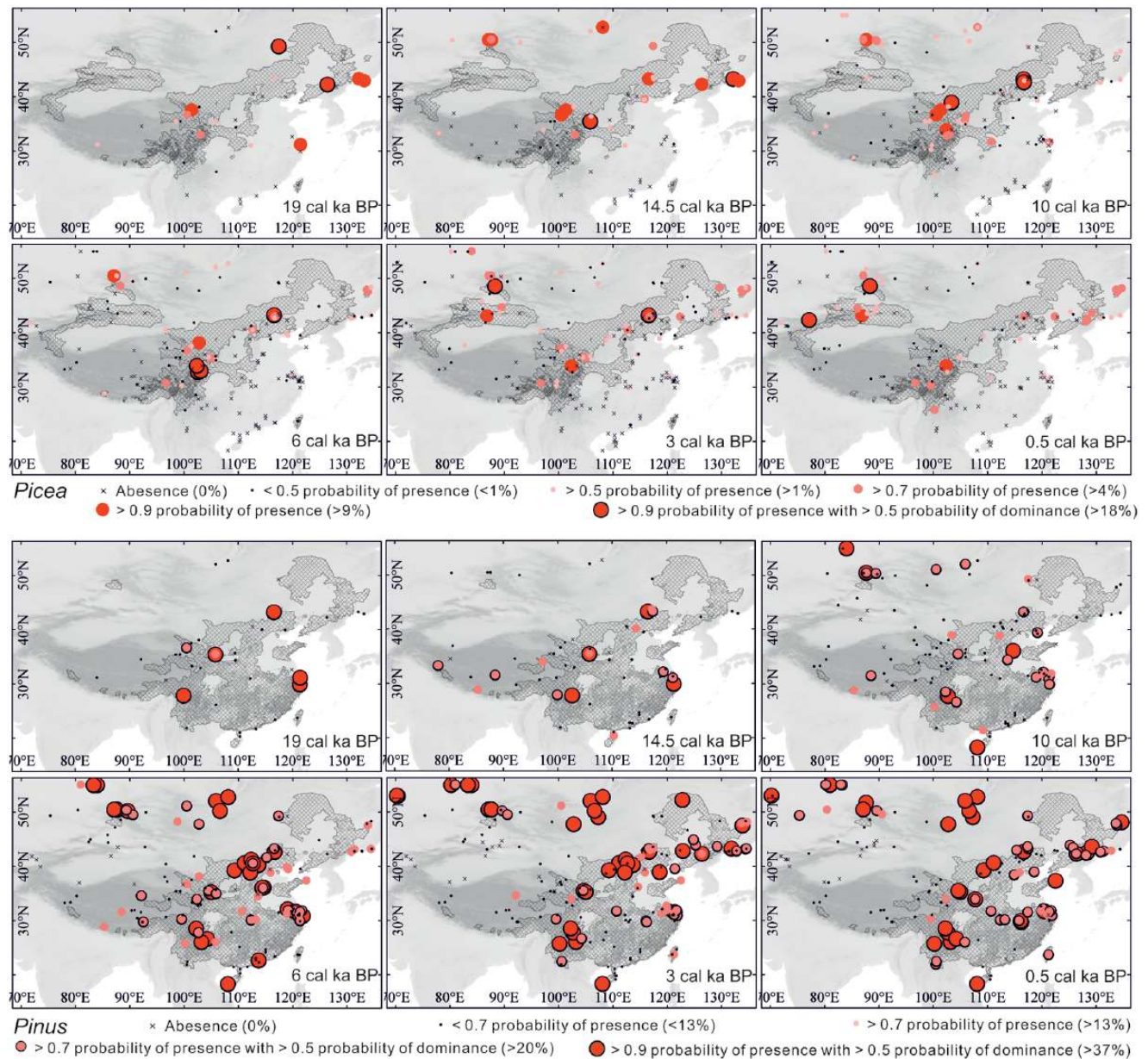


Figure 2. Spatial distributions of the 14 taxa at key time slices inferred by the pollen abundance and the pollen percentage threshold value. Grey hatching indicates the present geographical ranges (Fang et al., 2011), and the dark grey area shows the present distribution of dominant/indicative taxa (Hou, 2001).

and Zhujiang River during the last glacial period, and expanded to the middle reaches of the Yangtze River by about 9.5 kyr BP. After 3 kyr BP, chestnut tree abundance decreased markedly.

Castanopsis (Chinkapin). The distribution of chinkapin trees is restricted to the coastal areas of China during the LGM. From there, chinkapin trees expanded towards south-central China by 8 kyr BP where a first distribution centre formed from 7.5 to 3.5 kyr BP. The occurrence of chinkapin trees in the estuary of the Yangtze River was traced back to 12.5 kyr BP, and chinkapin trees spread to the middle reaches of the Yangtze River at 8 kyr BP where a second distribution centre formed, with remarkable increase in abundance in the 9–6 kyr BP interval. After 6 kyr BP, the abundance reduced noticeably in both distribution centres.

Cyclobalanopsis (Oriental White Oak). During the LGM, only a few sites from south-central China recorded the presence (>0.9 probability) of oriental white oak trees. After 14.5 kyr BP, oriental white oak trees increased in abundance and expanded inland into south-central China, achieving a maximum spatial extent between

c. 6 and 3 kyr BP in a belt from the Yangtze River Delta to the Yungui Plateau. After 6 kyr BP (particularly after 3 kyr BP), the abundance reduced noticeably.

Fagus (Beech). Beech trees survived only in one site from the Yungui Plateau in south-west China during the LGM. After 14 kyr BP, beech trees spread to the middle and lower reaches of the Yangtze River; the maximum abundance occurred between 2.5 and 1.5 kyr BP. After 1 kyr BP, beech tree abundance decreased markedly.

Pterocarya (Wingnut). Wingnut trees appeared with limited spatial extent in the Zhujiang River Delta between 16.5 and 12.5 kyr BP and after 10.5 kyr BP in the Yangtze River Delta.

Eurythermal broadleaved tree taxa

Juglans (Walnut). Walnut trees have three distribution centres after the LGM, located in the middle and lower reaches of the Yangtze River, the south-eastern Loess Plateau and mountainous areas of

north-central China, and Changbai Mountain and adjacent areas. Walnut trees survived in two sites from the Yungui Plateau and the middle reaches of the Yangtze River during the LGM. Its first distribution centre formed in the middle and lower reaches of the Yangtze River after 17.5 kyr BP, and reached its maximum spatial extent between 6.5 and 1.5 kyr BP. At 14.5 kyr BP, walnut trees appeared on the south-eastern Loess Plateau and Changbai Mountain, then expanded northward into the two distribution centres, with a maximum spatial extent during 9.5–6 kyr BP and 6.5–3 kyr BP, respectively. Walnut tree abundance in north-east and north-central China reduced markedly after 6 kyr BP.

Quercus (Oak). Oak tree presence is only recorded in the coastal areas of southern China and the Yangtze River Delta during the LGM. From 14.5 kyr BP, the distribution of oak trees expanded to the south-eastern rim of the Tibetan Plateau, into the coastal areas of the Russian Far East, and onto the Loess Plateau. Oak tree abundance reached a maximum by *c.* 6.5 kyr BP. After *c.* 3 kyr BP, oak tree abundance decreased throughout the study region, especially in northern and central China.

Tilia (Linden). Linden trees have two major distribution centres: one on Changbai Mountain and its adjacent areas, and a second in mountainous areas of north-central China. Linden trees appeared in the Yangtze River Delta at *c.* 19 kyr BP and at *c.* 15 kyr BP in north-central China where they reached their maximum abundance between 8.5 and 7.5 kyr BP. After 13 kyr BP, Linden trees appeared on Changbai Mountain, and then expanded north-eastward to the Russian Far East. Linden trees had their maximum spatial extent and abundance between 5.5 and 4.5 kyr BP. Linden tree abundances decreased markedly in north-central China and the Changbai Mountain areas after 6 kyr BP.

Ulmus (Elm). Elm trees were present in a few sites from present-day tropical and subtropical areas of China during the LGM, and the maximum in abundance occurred during the last deglaciation (14.5–11.5 kyr BP). Its appearance in north-central China occurred at 20 kyr BP and they flourished in the first half of the Holocene (*c.* 10–5 kyr BP). After 16.5 kyr BP, elm trees appeared on Changbai Mountain and spread north-eastward to adjacent areas during the last deglaciation, and flourished in the period 6–2.5 kyr BP. After 6 kyr BP, elm tree abundance in north-east and north-central China reduced markedly.

Cold-resistant broadleaved tree taxa

Betula (Birch). Birch trees have four major distribution centres located on Changbai Mountain and adjacent areas, the mountainous areas of north-central China, the south-eastern Tibetan Plateau and the north-western study region. Only a few pollen spectra (from Changbai Mountain and adjacent areas and the Lake Baikal area) reveal a continuous presence of birch trees during the LGM. Since the beginning of the Bølling/Allerød period (B/A; *c.* 14.5 kyr BP), the distribution areas of birch trees increased in the four centres and flourished on the south-eastern Tibetan Plateau during the early Holocene (10–9 kyr BP), in north-central China (8.5–7.5 kyr BP) and the north-western part of the study region in the mid-Holocene (8.5–3.5 kyr BP), and in the Changbai Mountain areas during the late Holocene (4.5–3 kyr BP). Birch tree abundance decreased in north-central China and on the south-eastern Tibetan Plateau during the late Holocene, particularly after 2 kyr BP.

Conifer taxa

Abies (Fir). Fir trees have two major distribution centres over the last 22 kyr: the south-eastern Tibetan Plateau and Changbai Mountain and adjacent areas. Three sites record fir trees throughout the

LGM: Qinling Mountain, the eastern Tibetan Plateau and Changbai Mountain. Fir trees spread to Hengduan Mountain and the south-eastern rim of the Tibetan Plateau, where the first distribution centre formed at around 14.5 kyr BP, and increased in abundance remarkably during the end of last deglaciation and early Holocene (12–9 kyr BP). Fir trees also invaded a few more sites in north-central China (16–10.5 kyr BP) and on Altai Mountain (10–0 kyr BP) but at low coverage and/or small spatial extent. The second distribution centre was established on Changbai Mountain and its adjacent areas after 5.5 kyr BP with increasing abundance, gradually expanding its range area until the present.

Larix (Larch). There are no pollen spectra indicating a continuous presence of larch trees during the period between 22 and 15.5 kyr BP. After 15 kyr BP, larch trees were steadily present in the Lake Baikal region and Altai Mountain, indicating a maximum spatial extent during the early Holocene (10.5–8.5 kyr BP).

Picea (Spruce). A first distribution centre formed on the north-eastern Tibetan Plateau rim during the Late Glacial period, and spruce trees spread to the west and the south after *c.* 13.5 kyr BP, having an early-to-mid-Holocene maximum and decreased in abundance markedly after *c.* 6 kyr BP.

From 17.5 kyr BP, spruce trees occurred continuously, and a spruce tree distribution centre formed around the Altai and Khangai mountains showing maximum abundance between 14 and 11.5 kyr BP. The presence of spruce trees around the Tianshan Mountain was *c.* 6500 years later than on Altai Mountain. Spruce trees were continually present in the mountainous areas of north-central China during the last 22 kyr. They increased after *c.* 14.5 kyr BP and reached their maximal spatial extent and abundance between 13 and 12 kyr BP, but they decreased markedly after *c.* 3 kyr BP. Spruce trees occurred in southern parts of the distribution centre located around Changbai Mountain throughout the last 22 kyr, and they spread to the northern parts by *c.* 6 kyr BP and reached their maximum extent and abundance there during the late Holocene.

Pinus (Pine). During the LGM, only a few sites record pine tree presence with high probabilities, such as the mountainous areas of north-central China, the Yangtze Delta, the south-western Loess Plateau and the south-eastern rim of the Tibetan Plateau. From *c.* 14.5 kyr BP, pine trees extended into surrounding areas. The distribution centre in east China reached a maximum abundance at *c.* 8 kyr BP. The area of pine trees extended on the eastern Tibetan Plateau after the beginning of the Holocene.

Pine trees appeared in the areas around the Altai, Khangai and Hentiy mountains from 14 kyr BP, where their maxima occurred during the late Holocene. Pine trees were absent in north-eastern parts of study region until about 8.5 kyr BP, but from that time on, their spatial extent and abundance increased and flourished in these areas after *c.* 3 kyr BP.

Discussion

Tree taxa distribution and abundance changes in space and time and their driving forces

Plant-macrofossil data of high taxonomic resolution are assumed to best document local vegetation composition, but vegetation reconstructions on a sub-continental scale in eastern North America derived from fossil pollen data have remarkable similarities to those obtained from macrofossil data (Jackson et al., 1997). Although there is no confirmatory macrofossil data for our region and available pollen records are sparse in the tropical and subtropical regions (which might cause a bias in representing tree distribution changes accurately), we are confident that the

arboreal distribution changes revealed by our fossil pollen dataset do roughly indicate the distribution changes of major tree taxa at a sub-continental scale in eastern continental Asia.

The present ranges of thermophilous broadleaved tree taxa (*Castanea*, *Castanopsis*, *Cyclobalanopsis*, *Fagus*, *Pterocarya*) are mostly restricted to tropical/subtropical regions of China. Their distribution (except for *Fagus* which only occurred on the Yungui Plateau) was restricted to the southern and south-eastern coastal areas of China during the LGM, where it was sufficiently warm and wet: LGM climate simulations (Jiang et al., 2011; Ju et al., 2007) suggest mean annual temperatures of about 11–16°C and annual precipitation of >900 mm for these areas. These taxa spread into the lower reaches of the Yangtze River during the B/A period or early Holocene. Their extent expanded westward into south-central China during the early Holocene and achieved their maximum distribution and highest abundance during the early or mid-Holocene, which correlates with the occurrence of the climate optimum in this area (Shi et al., 1993; Wang et al., 2005).

Based on syntheses of the temporal and spatial distributions of rice relic sites, Gong et al. (2007) suggest that early rice farming was widespread in the middle and lower reaches of the Yangtze River as well as throughout southern China during the late Holocene, which coincides with the decrease in tree abundances. Zheng et al. (2004) consider the decrease in tree abundance to be the result of the primitive ‘slash and burn’ method for land reclamation. Fuller and Qin (2010), however, suggest that the regional declines in nut-bearing trees (such as oak, chestnut and chinkapin) were the result of a cooling climatic event. In southern China, the late-Holocene precipitation was highest for the entire 20 kyr period (Liu et al., 2014) and the mean temperature of the current tropical/subtropical areas during the late Holocene was only about 1–2°C lower than during the mid-Holocene megathermal period (Shi et al., 1993; Zheng et al., 2004). Therefore, we think that climate cooling was unlikely to markedly reduce the spatial extent of these taxa, and the significant decrease in abundance throughout the current tropical/subtropical regions during the late Holocene is likely to have been caused by the destruction of forests by human activities instead.

Juglans, *Quercus*, *Tilia*, *Ulmus* have broad present-day ranges from the tropical/subtropical areas to the cool temperate area, and, in addition, *Ulmus* has a broad distribution in north-west China. During the LGM, these taxa were limited to the current tropical or subtropical regions (south of c. 30°N). They then spread northwards to north and north-east China and increased in abundance during the B/A period and early Holocene. They reached their maximum abundance and areal extent in eastern China during the mid-Holocene, reflecting the general climate-change patterns in the monsoonal regions of the study area (An et al., 2000; Shi et al., 1993; Wang et al., 2010).

During the late Holocene, *Quercus* abundance decreased in north-central China and the middle and lower reaches of the Yangtze River. North-central China is on the fringe of the East Asian Summer Monsoon area, and its natural ecosystem is highly sensitive to the summer monsoon migration (Qian et al., 2012). The weakening of the summer monsoon in the late Holocene has been confirmed by several studies based on various proxies (Shi et al., 1993; Wang et al., 2010; Zhang et al., 2011). During the late Holocene (after about 6 kyr BP), a decrease in *Quercus* abundance might be caused by the weak summer monsoon. However, decreases in *Quercus* abundance in the middle and lower reaches of the Yangtze River could be because of the destruction of forests by human activities (see discussion above). In addition, the cooling in the north-eastern part of the study region during the late Holocene might reduce the abundance of *Quercus* and *Tilia*.

Because of their cold resistance, *Abies*, *Betula*, *Picea* and *Pinus* have the broadest distribution ranges in the LGM among

the three groups. Climate simulations suggest that mean annual precipitation was 20–40% (or more) lower than today (Jiang et al., 2011; Shi et al., 1997) in north China and on the Tibetan Plateau. Low temperatures, but particularly the dry climate and the low atmospheric CO₂ in the LGM, may have contributed to the restricted distribution of forest, particularly in arid and high-elevation areas (Herzschuh et al., 2011; Levis et al., 1999). These taxa then increased in abundance and spread to surrounding areas since the last deglaciation, with no specific expansion direction.

Yang et al. (2010) discovered dune formation and activation in the Horqin dunefield from north-east China during the last glacial period, implying an arid late glacial period. Accordingly, the forest in the north-eastern study region was restricted to its southerly part during the last glacial period with *Picea* and *Betula* as the dominated components. Based on the synthesis of several palaeoclimate records, Shi et al. (1993) and An et al. (2000) infer the early-to-mid-Holocene to be warm and wet and the late Holocene to be cool and arid in this area. The eurythermal broadleaved taxa (*Juglans*, *Quercus*, *Tilia*, *Ulmus*) flourished during the early and mid-Holocene, and the conifer taxa (*Abies*, *Picea*, *Pinus*) abundances increased from the late Holocene (c. 6 kyr BP) and the modern temperate mixed conifer–deciduous broadleaved forest may have existed since then.

On the north-east rim of the Tibetan Plateau, *Picea* flourished during the B/A and the early Holocene, and *Betula* during the early and mid-Holocene, corresponding with increasing precipitation during the B/A period, and humid conditions in the early and mid-Holocene recorded by sediment redness from Qinghai Lake (Ji et al., 2005). Hence, precipitation should be an important driving force for forest expansion in this area. During the late Holocene, the regional decrease in abundance of *Picea* and *Betula* could result from the regional-scale climate drying event (Ji et al., 2005; Stauch et al., 2012). However, human impact, although not indicated in the scarce archaeological record, might also have contributed to forest decline (Schlütz and Lehmkuhl, 2009) but probably only at a local scale (Herzschuh et al., 2010), because of the enhanced human requirements for timber and agriculture.

Comparison of distribution change of trees between different continents

The major tree taxa in Europe, northern Eurasia and eastern North America show a consistent northward migration pattern because of warming and a moister climate since the LGM, as revealed by syntheses of fossil pollen and plant macrofossil data on continental scales (Binney et al., 2009; Brewer et al., 2002; Huntley and Birks, 1983; Jackson et al., 1997). In continental East Asia, the thermophilous and eurythermal broadleaved taxa have south-to-north expansion patterns generally similar to those in Europe, northern Eurasia and eastern North America, while the conifer taxa and *Betula* do not have distinct expansion directions. Additionally, the eurythermal broadleaved tree taxa have a slight westward spread with a shorter spatial range. Potential reasons for these different expansion patterns in our study region are as follows:

1. *The relatively narrow latitude-range of this study region.* In Europe, the northern limits of the glacial refugia for conifer taxa and *Betula* were at c. 43–63°N; these taxa spread northwards to limits north of their present ranges at c. 70°N during the Holocene (e.g. Binney et al., 2009; Feurdean et al., 2013). In eastern North America, the northern limits of conifer taxa and *Betula* during the full glacial period were at c. 45°N; these taxa spread northwards to c. 60°N after glacier retreats (Jackson et al., 1997). This study focuses on lower and middle latitudes, which were

relatively warm during the LGM compared with Europe and North America because of the continental climate and the lack of continental glaciers (Shi, 2005; Svendsen et al., 2004). Pollen mapping in the relatively narrow latitude-range fails to reveal the northward expansion pattern of these cold-resistant trees. In addition, in Europe and North America, complex expansion directions for cold-resistant trees were also noted for lower and middle latitudes (e.g. Bernabo and Webb, 1977; Van der Knaap et al., 2005), which support our findings.

2. *The geomorphological pattern.* The distribution of these conifer taxa and *Betula* were mostly restricted to the mountainous areas in our study. The microclimates caused by the varied topography might provide suitable habitats for trees (Taberlet and Cheddadi, 2002), which might also result in their wide distribution during the LGM. In addition, the lack of an east–west-stretching high mountain barrier in our study region, like the Alps in Europe (Van der Knaap et al., 2005), allowed fast tree spreading during a relatively warmer phase in the last glacial period, for example, the remarkably fast spread of *Quercus*, starting at the beginning of the B/A (after about 14.5 kyr BP) from southern China to the north-eastern rim of the Tibetan Plateau and north-central China. In contrast, *Quercus* was restricted to south of the Alps until the early Holocene (c. 11.5 kyr BP) in Europe (Brewer et al., 2002).
3. *The role of precipitation in tree migration patterns.* Huntley et al. (1995) suggest that temperature plays a key role in determining tree distributions in northern and central Europe, while moisture is the major determinant in southern Europe. Hence, major tree taxa were restricted to mid-elevation refugia in southern Europe (e.g. Bennett et al., 1991), which were warmer than higher latitudes (e.g. Barron and Pollard, 2002; Jost et al., 2005; Wright et al., 1993) and moister than the surrounding low plains (more orographic precipitation) during the LGM. This is in contrast to conditions in eastern continental Asia where the temperature gradient was not as steep but a strong precipitation gradient between coastal and inland areas existed because of the lack of a monsoonal circulation. Precipitation is still a major determinant of the present-day regional vegetation distribution (Fang et al., 2005; Hou, 1983), especially in arid/subarid areas (such as north-central China, the Loess Plateau and the Tibetan Plateau; Lu et al., 2011; Xu et al., 2010). Accordingly, in the arid/subarid area of northern China (35°–45°N, 110°–125°E), the eurythermal broadleaved taxa spread into the eastern parts of this area first (e.g. the coastal area and Changbai Mountain) during the B/A, and then spread into the western parts (e.g. the mountainous areas of north-central China and the northern part of the Loess Plateau) in the early or mid-Holocene. Hence, we infer that this westward expansion was related to the enhancement of the Asian Summer Monsoon during the early and mid-Holocene.

Implications for tree-range changes in the frame of global warming

From our study, the range expansion and/or abundance increase of all tree taxa occurred at the beginning of the B/A and the beginning of the early Holocene, at a time of the highest temperature and moisture increase rates during the last 22 kyr (Herzschuh, 2006; Wang et al., 2010). The westward expansion of the eurythermal broadleaved taxa into the arid/subarid areas suggests that precipitation plays a more important role than temperature in determining their distribution in these areas. The

observational and theoretical evidence implies that recent (and thus future) global warming causes weakening of the East Asian Summer Monsoon which leads to regional drought over northern China (Zhao et al., 2010; Zhu et al., 2012). The drying climatic conditions could cause shrinkage in the range of eurythermal broadleaved taxa (*Juglans*, *Quercus*, *Tilia* and *Ulmus*) in the arid/subarid areas, adding to the loss of forests in these areas from past and recent human impact. However, the ‘Grain for Green Project’ initiated by the Chinese government in 1999 has already yielded some forest restoration success especially in the northern forest-steppe transitional areas (Li et al., 2013). There is thus a chance that enhanced environmental awareness and active forest restoration will foster the extension and densification of the remaining forest fragments, even against a background of drier climatic conditions.

Conclusion

Our investigation of 14 key arboreal taxa has revealed significant changes in their spatial and temporal distributions. The changes are a reflection of both climate dynamics and historical human activity. The tree expansion patterns are different from those in Europe and North America, not only because of the specific environmental setting (i.e. the lack of inland glaciers during the LGM and of east–west stretching mountain ranges as well as the limiting effect of moisture) but also because of (the still not fully quantifiable) human impact. Based on our study, we can forecast that drying in the areas of the East Asian Summer Monsoon, as predicted by climate studies, would cause shrinkage of the total area suitable for eurythermal broadleaved taxa. Forest loss, however, may be compensated if reforestation projects within the prospective areas of the climatic niche of these taxa are successful.

Acknowledgements

Ulrike Herzschuh and Yan Zhao thank H John B. Birks for his long-term support of their scientific careers.

Funding

This study was supported by the German Research Foundation (DFG) and the National Natural Science Foundation of China (NSFC). The doctoral research of Xianyong Cao is funded by the ‘Helmholtz–China Scholarship Council (CSC) Young Scientist Fellowship’ (No. 20100813031). Cathy Jenks provided linguistic help.

References

- An Z, Porter SC, Kutzbach JE et al. (2000) Asynchronous Holocene optimum of the East Asian monsoon. *Quaternary Science Reviews* 19: 743–762.
- Barron E and Pollard D (2002) High-resolution climate simulations of oxygen isotope stage 3 in Europe. *Quaternary Research* 58: 296–309.
- Bennett KD, Tzedakis PC and Willis KJ (1991) Quaternary refugia of north European trees. *Journal of Biogeography* 18: 103–115.
- Bernabo JC and Webb T III (1977) Changing patterns in the Holocene pollen record of northeastern North America: A mapped summary. *Quaternary Research* 8: 64–96.
- Binney HA, Willis KJ, Edwards ME et al. (2009) The distribution of late-Quaternary woody taxa in northern Eurasia: Evidence from a new macrofossil database. *Quaternary Science Reviews* 28: 2445–2464.
- Blaauw M and Christen JA (2011) Flexible paleoclimate age-depth models using an autoregressive gamma process. *Bayesian Analysis* 6: 457–474.

- Brewer S, Cheddadi R, de Beaulieu JL et al. (2002) The spread of deciduous *Quercus* throughout Europe since the last glacial period. *Forest Ecology and Management* 156: 27–48.
- Campo EV and Gasse F (1993) Pollen- and diatom-inferred climatic and hydrological changes in Sumxi Co Basin (Western Tibet) since 13,000 yr B.P. *Quaternary Research* 39: 300–313.
- Cao XY, Ni J, Herzschuh U et al. (2013) A late Quaternary pollen dataset from eastern continental Asia for vegetation and climate reconstructions: Set up and evaluation. *Review of Palaeobotany and Palynology* 194: 21–37.
- Fang JY, Wang ZH and Tang ZY (2011) *Atlas of Woody Plants in China: Distribution and Climate (Volume 1)*. Beijing: Higher Education Press, and Berlin: Springer-Verlag.
- Fang JY, Piao SL, Zhou LM et al. (2005) Precipitation patterns alter growth of temperature vegetation. *Geophysical Research Letters* 32: 411–415.
- Feurdean A, Bhagwat SA, Willis KJ et al. (2013) Tree migration rates: Narrowing the gap between inferred post-glacial rates and projected rates. *PLoS ONE* 8: e71797.
- Fu C (2003) Potential impacts of human-induced land cover change on East Asia Monsoon. *Global and Planetary Change* 37: 219–229.
- Fuller DQ and Qin L (2010) Declining oaks, increasing artistry, and cultivating rice: The environmental and social context of the emergence of farming in the Lower Yangtze Region. *Environmental Archaeology* 15: 139–159.
- Giesecke T and Bennett KD (2004) The Holocene spread of *Picea abies* (L.) Karst. in Fennoscandia and adjacent areas. *Journal of Biogeography* 31: 1523–1548.
- Gong Z, Zhang X, Chen J et al. (2003) Origin and development of soil science in ancient China. *Geoderma* 115: 3–13.
- Gong ZT, Chen HZ, Yuan DG et al. (2007) The temporal and spatial distribution of ancient rice in China and its implications. *Chinese Science Bulletin* 52: 1071–1079.
- Herzschuh U (2006) Palaeo-moisture evolution at the margins of the Asian monsoon during the last 50 kyr. *Quaternary Science Reviews* 25: 163–178.
- Herzschuh U, Birks HJB, Ni J et al. (2010) Holocene land-cover changes on the Tibetan Plateau. *The Holocene* 20: 91–104.
- Herzschuh U, Ni J, Birks HJB et al. (2011) Driving forces of mid-Holocene vegetation shifts on the upper Tibetan Plateau, with emphasis on changes in atmospheric CO₂ concentrations. *Quaternary Science Reviews* 30: 1907–1917.
- Hilbig W (1995) *The Vegetation of Mongolia*. Amsterdam: SPB Academic Publishing.
- Hou X (2001) *Vegetation Atlas of China*. Beijing: Science Press.
- Huntley B and Birks HJB (1983) *An Atlas of Past and Present Pollen Maps for Europe: 0–13000 Years Ago*. Cambridge: Cambridge University Press.
- Huntley B, Berry PM, Cramer W et al. (1995) Modelling present and potential future ranges of some European higher plants using climate response surfaces. *Journal of Biogeography* 22: 967–1001.
- Jackson ST, Overpeck JT, Webb T, III et al. (1997) Mapped plant-macrofossil and pollen records of late Quaternary vegetation change in eastern North America. *Quaternary Science Reviews* 16: 1–70.
- Ji J, Shen J, Balsam W et al. (2005) Asian monsoon oscillations in the northeastern Qinghai-Tibet Plateau since the late glacial as interpreted from visible reflectance of Qinghai Lake sediments. *Earth and Planetary Science Letters* 233: 61–70.
- Jiang D, Lang X, Tian Z et al. (2011) Last glacial maximum climate over China from PMIP simulations. *Palaeogeography, Palaeoclimatology, Palaeoecology* 309: 347–357.
- Jost A, Lunt D, Kageyama M et al. (2005) High-resolution simulations of the last glacial maximum climate over Europe: A solution to discrepancies with continental palaeoclimatic reconstructions? *Climate Dynamics* 24: 577–590.
- Ju L, Wang H and Jiang D (2007) Simulation of the Last Glacial Maximum climate over East Asia with a regional climate model nested in a general circulation model. *Palaeogeography, Palaeoclimatology, Palaeoecology* 248: 376–390.
- Krengel M (2000) Discourse on history of vegetation and climate in Mongolia-palynological report of sediment core Bayan Nuur I (NW-Mongolia). In: Walther M, Janzen J, Riedel F et al. (eds) *State and Dynamics of Geosciences and Human Geography in Mongolia: Extended Abstracts of the International Symposium* (Berliner Geowissenschaftliche Abhandlungen), Berlin: Selbstverlag Fachbereich Geowissenschaften, pp. 80–84.
- Levis S, Foley JA and Pollard D (1999) CO₂, climate, and vegetation feedbacks at the Last Glacial Maximum. *Journal of Geophysical Research* 104: 31191–31198.
- Li S, Yan J, Liu X et al. (2013) Response of vegetation restoration to climate change and human activities in Shaanxi-Gansu-Ningxia region. *Journal of Geographical Sciences* 23: 98–112.
- Li X, Dodson J, Zhou J et al. (2009) Increases of population and expansion of rice agriculture in Asia, and anthropogenic methane emissions since 5000 BP. *Quaternary International* 202: 41–50.
- Liu Z, Wen X, Brady EC et al. (2014) Chinese cave records and the East Asia Summer Monsoon. *Quaternary Science Reviews* 83: 115–128.
- Lu H, Wu N, Liu K-B et al. (2011) Modern pollen distributions in Qinghai-Tibetan Plateau and the development of the transfer functions for reconstructing Holocene environmental changes. *Quaternary Science Reviews* 30: 947–966.
- Lu H, Zhang J, Liu K-B et al. (2009) Earliest domestication of common millet (*Panicum miliaceum*) in East Asia extended to 10,000 years ago. *Proceedings of the National Academy of Sciences of the United States of America* 106: 7367–7372.
- Olson DM, Dinerstein E, Wikramanayake ED et al. (2001) Terrestrial ecoregions of the world: A new map of life on Earth. *BioScience* 51: 933–938.
- Paillard D, Labeyrie L and Yiou P (1996) Macintosh program performs time-series analysis. *EOS Transactions* 77: 379.
- Qian W, Shan X, Chen D et al. (2012) Droughts near the northern fringe of the East Asian summer monsoon in China during 1470–2003. *Climatic Change* 110: 373–383.
- Ren G (2007) Changes in forest cover in China during the Holocene. *Vegetation History and Archaeobotany* 16: 119–126.
- Ren G and Beug HJ (2002) Mapping Holocene pollen data and vegetation of China. *Quaternary Science Reviews* 21: 1395–1422.
- Ren G and Zhang L (1998) A preliminary mapped summary of Holocene pollen data for Northeast China. *Quaternary Science Reviews* 17: 669–688.
- Schlütz F and Lehmkuhl F (2009) Holocene climatic change and the nomadic Anthropocene in Eastern Tibet: Palynological and geomorphological results from the Nianbaoyeze Mountains. *Quaternary Science Reviews* 28: 1449–1471.
- Shi Y (2005) *The Quaternary Glaciations and Environmental Variations in China*. Shijiazhuang: Hebei Science and Technology Press. (In Chinese)
- Shi Y, Zheng B and Yao T (1997) Glaciers and environments during the Last Glacial Maximum (LGM) on the Tibetan Plateau. *Journal of Glaciology and Geocryology* 19: 97–113. (In Chinese)
- Shi Y, Kong Z, Wang S et al. (1993) Mid-Holocene climates and environments in China. *Global and Planetary Change* 7: 219–233.
- Stauch G, Lehmkuhl F, Hilgers A et al. (2012) Holocene aeolian sediments on the NE Tibetan Plateau. In: *Geophysical Research Abstracts (EGU)*. Göttingen: Copernicus, p. 7491.

- Svendsen JI, Alexanderson H, Astakhov VI et al. (2004) Late Quaternary ice sheet history of northern Eurasia. *Quaternary Science Reviews* 23: 1229–1271.
- Taberlet P and Cheddadi R (2002) Quaternary refugia and persistence of biodiversity. *Science* 297: 2009–2010.
- Tao SY and Chen LX (1987) A review of recent research on the East Asian summer monsoon in China. In: Chang CP and Krishnamurti TN (eds) *Monsoon Meteorology*. Oxford: Oxford University Press, pp. 60–92.
- Van der Knaap WO, van Leeuwen JFN, Finsinger W et al. (2005) Migration and population expansion of *Abies*, *Fagus*, *Picea*, and *Quercus* since 15000 years in and across the Alps, based on pollen-percentage threshold values. *Quaternary Science Reviews* 24: 645–680.
- Wang Y, Liu X and Herzschuh U (2010) Asynchronous evolution of the Indian and East Asian Summer Monsoon indicated by Holocene moisture patterns in monsoonal central Asia. *Earth Science Reviews* 103: 135–153.
- Wang Y, Cheng H, Edwards RL et al. (2005) The Holocene Asian monsoon: Links to solar changes and North Atlantic climate. *Science* 308: 854–857.
- Wang Y, Herzschuh U, Shumilovskikh LS et al. (2014) Quantitative reconstruction of precipitation changes on the NE Tibetan Plateau since the Last Glacial Maximum – Extending the concept of pollen source area to pollen-based climate reconstructions from large lakes. *Climate of the Past* 10: 21–39.
- Wright HE, Kutzbach JE, Webb T, III et al. (1993) *Global Climates since the Last Glacial Maximum*. Minneapolis, MN: University of Minnesota Press.
- Xu Q, Li Y, Bunting MJ et al. (2010) The effects of training set selection on the relationship between pollen assemblages and climate parameters: Implications for reconstructing past climate. *Palaeogeography, Palaeoclimatology, Palaeoecology* 289: 123–133.
- Yang LH, Zhou J, Lai ZP et al. (2010) Lateglacial and Holocene dune evolution in the Horqin dunefield of northeastern China based on luminescence dating. *Palaeogeography, Palaeoclimatology, Palaeoecology* 296: 44–51.
- Yoon SO, Kim HR, Hwang S et al. (2011) Holocene vegetation and climatic change inferred from isopollen maps on the Korean Peninsula. *Quaternary International* 254: 58–67.
- Zhang JR, Jia YL, Lai ZP et al. (2011) Holocene evolution of Huangqihai Lake in semi-arid northern China based on sedimentology and luminescence dating. *The Holocene* 21: 1261–1268.
- Zhao P, Yang S and Yu R (2010) Long-term changes in rainfall over eastern China and large-scale atmospheric circulation associated with recent global warming. *Journal of Climate* 23: 1544–1562.
- Zheng Z, Deng Y, Zhang H et al. (2004) Holocene environmental changes in the tropical and subtropical areas of the South China and the relation to human activities. *Quaternary Sciences* 24: 387–393. (In Chinese)
- Zhou XY and Li XQ (2012) Variations in spruce (*Picea* sp.) distribution in the Chinese Loess Plateau and surrounding areas during the Holocene. *The Holocene* 22: 687–696.
- Zhu C, Wang B, Qian W et al. (2012) Recent weakening of the northern East Asian summer monsoon: A possible response to global warming. *Geophysical Research Letters* 39: L09701.